

Remote Hydrogen Plasma Chemical Vapor Deposition from (Dimethylsilyl)(trimethylsilyl)methane. 1. Kinetics of the Process; Chemical and Morphological Structure of Deposited Silicon–Carbon Films

A. M. Wróbel* and A. Walkiewicz-Pietrzykowska

Centre of Molecular and Macromolecular Studies, Polish Academy of Sciences,
Sienkiewicza 112, PL-90-363 Łódź, Poland

J. E. Klemberg-Sapieha

Groupe des Couches Minces and Department of Engineering Physics, Ecole Polytechnique,
Montreal, Quebec H3C 3A7, Canada

Y. Nakanishi, T. Aoki, and Y. Hatanaka

Research Institute of Electronics, Shizuoka University, Hamamatsu 432, Japan

Received July 3, 2002. Revised Manuscript Received December 16, 2002

Amorphous hydrogenated silicon–carbon (a-Si:C:H) films have been produced by the remote hydrogen plasma chemical vapor deposition (RHP-CVD) using (dimethylsilyl)-(trimethylsilyl)methane as a single-source compound. The effect of the substrate temperature on the kinetics of the RHP-CVD process, structure, composition, and surface morphology of the resulting film has been investigated. The Arrhenius plots of substrate temperature dependencies of the mass- and thickness-based film growth rate imply that the investigated RHP-CVD is an adsorption-controlled process. The increase of the substrate temperature from 30 to 400 °C causes the elimination of organic moieties from the film and the formation of a Si-carbide network structure. The microscopic examination revealed that the films are defect-free materials of excellent morphological homogeneity and good conformality of coverage.

1. Introduction

Among the various CVD methods used for the fabrication of a-Si:C:H films, remote hydrogen plasma CVD (RHP-CVD) is a relatively novel and extremely useful technique offering well-controlled deposition conditions, free of film-damaging effects, such as charged-particle bombardment or high-energy ultraviolet irradiation,^{1–4} which are inherently involved in the direct plasma CVD (DP-CVD).⁵ This technique substantially differs from the conventional DP-CVD in two major aspects. The first is that the plasma generation and film deposition takes place in spatially separated regions. Second is that the plasma is induced in a region free of a source compound, unlike DP-CVD, using a non-film-forming gas, that is, hydrogen. The electrically neutral hydrogen atoms,

effectively generated in the hydrogen plasma, are fed, through the remote section (trap for the electrons, ions, excited atoms, and photons), to the CVD reactor. Thereby, RHP-CVD is exclusively induced via chemical reaction between the uncharged, ground-state hydrogen atoms and the source compound molecules, resulting in the formation of only radical active species. In contrast, the electron impact predominating in DP-CVD involves strong fragmentation of the molecules into a variety of radical, ionic, and neutral active species. Moreover, a significantly lower concentration of active species contributing to RHP-CVD, compared to that of DP-CVD, reduces markedly the growth step in the gas phase, thus preventing the formation of powder particles, which often contaminate the DP-CVD films. Due to these beneficial features, RHP-CVD is very promising for the production of defect-free a-Si:C:H thin-film materials.^{4,6–11}

* To whom correspondence should be addressed. E-mail: amwrobel@bilbo.cbmm.lodz.pl.

(1) Lucovsky, G.; Tsu, D. V.; Rudder, R. A.; Markunas, R. J. In *Thin Film Processes II*; Vossen, J. L., Kern, W., Eds.; Academic: Boston, MA, 1991; Chapter 4.2.

(2) Luft, W.; Tsuo, Y. *Hydrogenated Amorphous Silicon Alloy Deposition Process*; Marcel Dekker: New York, 1993; Chapter 9.

(3) Wróbel, A. M.; Wickramanayaka, S.; Hatanaka, Y. *J. Appl. Phys.* **1994**, *76*, 558.

(4) Wróbel, A. M.; Wickramanayaka, S.; Nakanishi, Y.; Hatanaka, Y.; Wysiecki, M. *J. Chem. Vap. Deposition* **1994**, *2*, 229.

(5) Wróbel, A. M.; Czeremuszkin, G. *Thin Solid Films* **1992**, *216*, 203.

(6) Wróbel, A. M.; Wickramanayaka, S.; Nakanishi, Y.; Fukuda, Y.; Hatanaka, Y. *Chem. Mater.* **1995**, *7*, 1403.

(7) Wróbel, A. M.; Wickramanayaka, S.; Nakanishi, Y.; Hatanaka, Y. *J. Mater. Process. Technol.* **1995**, *53*, 477.

(8) Wróbel, A. M.; Wickramanayaka, S.; Nakanishi, Y.; Hatanaka, Y.; Pawlowski, S.; Olejniczak, W. *Diamond Relat. Mater.* **1997**, *6*, 1081.

(9) Wróbel, A. M.; Wickramanayaka, S.; Kitamura, K.; Nakanishi, Y.; Hatanaka, Y. *Chem. Vap. Deposition* **2000**, *6*, 315.

(10) Hatanaka, Y.; Sano, K.; Aoki, T.; Wróbel, A. M. *Thin Solid Films* **2000**, *368*, 287.

(11) Wróbel, A. M. *J. Phys. IV France* **2001**, *11Pr3*, 691.

On the basis of the results of our earlier study^{12,13} on the reactivity of the alkylsilane and alkylcarbosilane precursors in an atomic hydrogen environment, we have selected (dimethylsilyl)(trimethylsilyl)methane (DTMSM), $\text{Me}_3\text{SiCH}_2\text{SiHMe}_2$, as a single-source compound very effective for the production of a-Si:C:H films by RHP-CVD. The yield of the RHP-CVD process involving DTMSM was found to be much higher than those of the alkylsilane compounds (e.g., trimethylsilane, hexamethyldisilane).¹³ This is due to DTMSM's easy conversion to 1,1-dimethylsilene, $\text{Me}_2\text{Si}=\text{CH}_2$, transient intermediate, which is highly reactive film-forming precursor.¹³ It is noteworthy that DTMSM,^{14,15} as well as other carbosilane compounds of linear and branched molecular skeletons, such as bis(trimethylsilyl)methane (BTMSM),¹⁶ disilylmethane,^{17–20} trisilylmethane,^{18–21} and tetrasilylmethane,^{18–20} respectively, was used as the a-Si:C:H film precursors in DP-CVD. However, the DP-CVD process, contrary to RHP-CVD, is insensitive to the molecular structure of the source compound. This is well-illustrated by the results of comparative DP-CVD experiments, which showed that DTMSM and BTMSM form films with nearly the same yields.¹⁴ On the other hand, inability of the latter compound to form film by RHP-CVD¹³ indicates that the C–H and Si–C bonds are inactive in the initiation step and the process involving DTMSM is induced with an exclusive contribution of the Si–H bonds.^{12,13} Due to high reactivity of the Si–H bonds with atomic hydrogen, DTMSM was found to undergo easy conversion to the a-Si:C:H film-forming precursors.¹³

In the present paper we characterize the kinetics of the RHP-CVD process involving the DTMSM source compound and resulting a-Si:C:H films using the various spectroscopic and microscopic techniques. In particular, the effect of the substrate (or deposition) temperature on the growth rate of the a-Si:C:H film and its chemical structure, composition, and surface morphology is reported. The results of this structural study are very useful for determining the relationships between the film structure and its physical, mechanical, and optical properties, which are the subject of the second part of this work.

2. Experimental Section

2.1. Remote Plasma CVD System and Film Growth Conditions. The remote plasma CVD system used for the production of the a-Si:C:H films, described earlier,²² consists

(12) Wróbel, A. M.; Walkiewicz-Pietrzykowska, A.; Stasiak, M.; Aoki, T.; Hatanaka, Y.; Szumilewicz, J. *J. Electrochem. Soc.* **1998**, *145*, 1060.

(13) Wróbel, A. M.; Walkiewicz-Pietrzykowska, A. *Chem. Vap. Deposition* **1998**, *4*, 133.

(14) Wróbel, A. M.; Stańczyk, W. *Chem. Mater.* **1994**, *6*, 1766.

(15) Wróbel, A. M.; Walkiewicz-Pietrzykowska, A. *J. Chem. Vap. Deposition* **1995**, *4*, 87.

(16) Inagaki, N.; Kondo, S.; Hirata, M.; Urushibata, H. *J. Appl. Polym. Sci.* **1985**, *30*, 3385.

(17) Beyer, W.; Hager, R.; Schmidbaur, H.; Winterling, G. *Appl. Phys. Lett.* **1989**, *54*, 1666.

(18) Folsch, J.; Rubel, H.; Schade, H. *Appl. Phys. Lett.* **1992**, *61*, 3029.

(19) Folsch, J.; Rubel, H.; Schade, H. *J. Appl. Phys.* **1993**, *73*, 8485.

(20) Rubel, H.; Folsch, J.; Schade, H. *Solid State Comm.* **1993**, *85*, 593.

(21) Li, Y.-M.; Fieselmann, B. F. *Appl. Phys. Lett.* **1991**, *59*, 1720.

(22) Wróbel, A. M.; Walkiewicz-Pietrzykowska, A.; Hatanaka, Y.; Wickramanayaka, S.; Nakanishi, Y. *Chem. Mater.* **2001**, *13*, 1884.

of three major parts: a plasma generation section (made of Pyrex glass tube, 28 mm i.d.) coupled via a resonant cavity and a waveguide with a 2.45-GHz microwave power supply unit; a remote section equipped with a Wood's horn photon trap; a CVD reactor (made of Pyrex glass by HWS, Mainz) containing greaseless conical joints, 20-cm-diameter flat flanges sealed with an O-ring, and stainless steel 13-cm-diameter substrate holder equipped with a heater. A source compound injector (4 mm i.d.) is located approximately 4 cm in front of the substrate holder. Deposition experiments were performed at a total pressure of $p = 0.56$ Torr (75 Pa), hydrogen flow rate $F(\text{H}_2) = 100$ sccm, microwave power input $P = 150$ W, and substrate temperatures $T_s = 30$ –400 °C. The DTMSM source compound was fed into the CVD reactor at the evaporation temperature of 20 °C with the flow (or feeding) rate $F(\text{DTMSM}) = 3.9$ mg min⁻¹ = 0.6 sccm. The flow rate of hydrogen was controlled using a MKS mass flow controller. In the case of the source compound, a mass flow controller was used to maintain a constant flow and the flow rate was estimated gravimetrically. Concentration of the atomic hydrogen in the CVD reactor, determined previously¹² by the NO₂ titration method, was $[\text{H}] = 5 \times 10^{15}$ cm⁻³ and its feeding rate $F(\text{H}) = 27$ sccm.¹² Using the last value and the flow rate of the source compound $F(\text{DTMSM}) = 0.6$ sccm, we evaluated the approximate number of hydrogen atoms (N_{H}) per single molecule of the source compound as $N_{\text{H}} = F(\text{H})/F(\text{DTMSM}) \approx 60$ atom/molecule. Films were deposited on one-side of polished p-type crystalline silicon (c-Si) wafers used as a model substrate for spectroscopic analyses and on Fisher microscope cover glass plates (45 × 50 × 0.2 mm) for the determination of the film mass. Prior to film deposition, the substrates were cleaned by successive rinsing with hexane, acetone, and deionized water. The c-Si wafers were additionally treated with a diluted hydrofluoric acid, rinsed with deionized water, and finally dried in an argon ambient. The deposition time was 60–120 min and thickness of the deposited films ranged from 0.7 to 1 μm. To evaluate the experimental reproducibility, at least three film depositions were carried out at fixed conditions. The distance between the plasma edge and the source compound inlet was 30 cm. No deposition was observed in the plasma region, indicating that there was no back diffusion of a source compound.

2.2. Spectroscopic and Related Techniques. Fourier transform infrared (FTIR) absorption spectra of the DTMSM source compound and the a-Si:C:H films, deposited on c-Si wafers, were recorded in the transmission mode on a FTIR-Infinity ATI Matson spectrophotometer. The spectrum of the PMDSM liquid source compound was recorded for about 0.1-mm-thick liquid film. Deconvolution of the FTIR absorption envelopes into individual absorption bands was performed using Gaussian functions for curve fitting.

X-ray photoelectron spectra (XPS) of the films were run on a VG-ESCALAB 3 Mark II surface analytical instrument using Mg K α X-rays as the photoexcitation source with an electron takeoff angle of 45° from the surface normal. Prior to the XPS analysis, the surface of the film sample was cleaned by sputter-etching with a 1-kV Ar⁺ beam. Curve fitting with mixed Gaussian/Lorentzian functions was performed on unsmoothed data following background subtraction.

Auger electron spectroscopic (AES) analysis was performed by means of an ULVAC AQM 808 system. The films were subjected to sputter-etching with a 2-kV Ar⁺ beam prior to the analysis and the AE spectra were recorded for the bulk region at a depth of about 100 nm. The atomic composition of the films was determined from the intensity of doubly integrated AES bands using the sensitivity factors 0.35, 0.18, and 0.50 for Si, C, and O, respectively.

Thickness of the films deposited on c-Si wafers was measured ellipsometrically using a Nippon Infrared Industrial Co. EL-101D ellipsometer equipped with a 632.8-nm He–Ne laser.

2.3. Microscopic Examination. Surface morphology of the films deposited on the c-Si substrate was examined by scanning electron microscopy (SEM) using a JEOL JSM 6100 electron microscope and atomic force microscopy (AFM) using a TopoMetrix TMX 2010 instrument. AFM examinations were

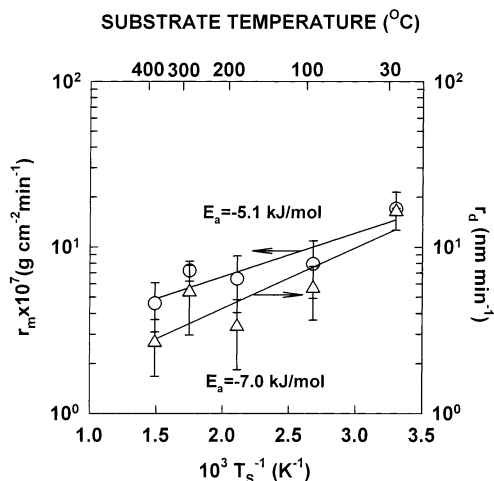


Figure 1. Mass- and thickness-based growth rates of the a-Si:C:H film, r_m (○) and r_d (△), respectively, as a function of inverse substrate temperature T_s .

performed at room temperature in air. To evaluate conformality of coverage, the films were deposited onto Al trapezoidal trench and tapered cavity patterns, sized on the micrometer scale, and then examined by SEM.

2.4. Materials. The DTMSM source compound was synthesized in our laboratory according to the procedure in ref 23; its purity, as checked by gas chromatography, was better than 99%. The hydrogen upstream gas was of 99.99% purity.

3. Results and Discussion

3.1. Kinetics of Film Growth. Figure 1 shows the effect of thermal activation on the kinetics of RHP-CVD characterized by the substrate temperature dependencies of the mass- and thickness-based film growth rates, r_m and r_d , respectively, determined in the form of the Arrhenius plots. The negative values of the apparent activation energy $E_a = -5.1$ kJ mol⁻¹ and $E_a = -7.0$ kJ mol⁻¹, resulting from the slopes of the r_m and r_d Arrhenius plots, respectively, imply that the RHP-CVD is mainly controlled by the adsorption of film-forming precursors from the gas phase onto the growth surface. In this case, the apparent activation energy is expressed as $E_a = E_r + \Delta E_{ad}$, where E_r denotes the activation energy of the film-forming reaction and ΔE_{ad} is the apparent heat of adsorption of the film-forming precursors and has a negative value.^{24,25} Thus, the negative E_a values is due to the fact that the absolute ΔE_{ad} value is higher than the E_r value. These results account for the adsorption of the precursors onto the growth surface as the major factor limiting the film growth rate. An analogous thermal activation effect, exhibiting $E_a < 0$, has been observed for remote oxygen plasma CVD²⁵ and DP-CVD^{26–30} involving a number of organosilicon source compounds.

3.2. Film Structure. *FTIR Spectroscopy.* The FTIR spectra of the a-Si:C:H films deposited at various substrate temperatures are presented in Figure 2 which shows, for comparison, also the spectrum of the DTMSM source compound. The assignment of particular absorption bands was based on the literature data.^{31–34} As can

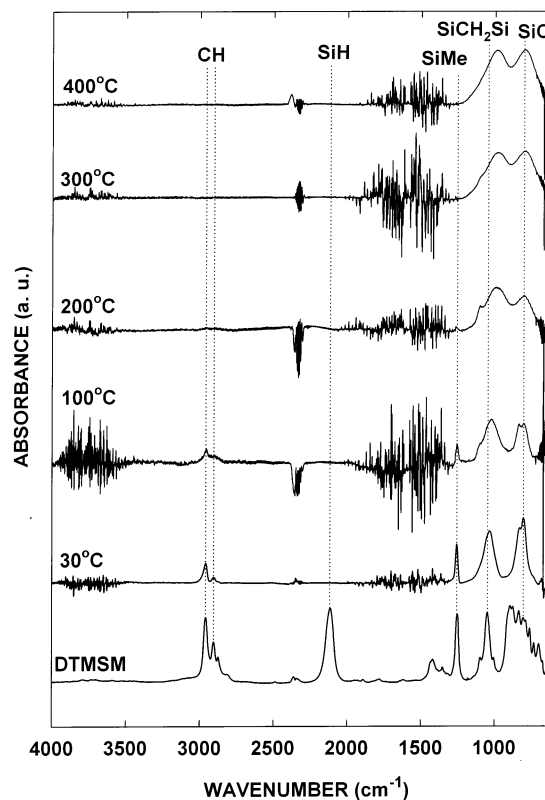


Figure 2. FTIR transmission spectra of liquid film of the DTMSM source compound and the a-Si:C:H films deposited on a c-Si substrate at various deposition temperatures $T_s = 30, 100, 200, 300,$ and 400 °C.

be noted from Figure 2, film spectra reveal the presence of broad absorption bands with a maximum in the range of 1030–1000 cm⁻¹ and 804–801 cm⁻¹, characteristic of carbosilane Si–CH₂–Si and carbidic Si–C units,^{32–34} respectively. The first band (1040–1000 cm⁻¹) may be interfered with the absorption arising from Si–O–Si and/or Si–O–C linkages, which also fall in this region. The Si–CH₂–Si band is very distinct in the spectrum of DTMSM and falls at 1048 cm⁻¹. The shift of a maximum position of this band toward a lower wavenumber range (1040–1000 cm⁻¹) in the film spectra is due to a different chemical environment of the Si–CH₂–Si unit in the a-Si:C:H film with respect to the DTMSM molecule. Weak intensity bands in the range 2960–2900 cm⁻¹ are attributed to C–H stretching mode in CH_{*n*} (*n* = 1–3) groups. A narrow and low-intensity band at 1260 cm⁻¹ originates from –Me deformation mode in the SiMe_{*n*} (*n* = 1–3) groups. An interesting feature of the film spectra in Figure 2 is the lack of the absorption

(26) Secrist, D. R.; Mackenzie, J. D. *J. Electrochem. Soc.* **1966**, *113*, 914.

(27) Emesh, I. T.; d'Asti, G.; Mercier, J. S.; Leung, P. *J. Electrochem. Soc.* **1989**, *136*, 3404.

(28) Wróbel, A. M.; Kryszewski, M. *Prog. Colloid Polym. Sci.* **1991**, *85*, 91.

(29) Favia, P.; Lamendola, R.; d'Agostino, R. *Plasma Sources Sci. Technol.* **1992**, *1*, 59.

(30) Niemann, J.; Bauhofer, W. *Thin Solid Films* **1999**, *352*, 249.

(31) Anderson, D. R. In *Analysis of Silicones*; Smith, A. L., Ed.; Wiley-Interscience: New York, 1974; Chapter 10.

(32) Tsai, H.-K.; Lin, W.-L.; Sah, W. J.; Lee, S.-C. *J. Appl. Phys.* **1988**, *64*, 1910.

(33) Deplancke, M. P.; Powers, J. M.; Vandentop, G. J.; Salmeron, M.; Somorjai, G. A. *J. Vac. Sci. Technol.* **1990**, *A9*, 450.

(34) Bhusari, D. M.; Kshirsagar, S. T. *J. Appl. Phys.* **1993**, *73*, 1743.

(23) Graber, G.; Degler, G. *Chem. Abstr.* **1962**, *57*, 12526i.

(24) Raupp, G. B.; Shemansky, F. A.; Cale, T. S. *J. Vac. Sci. Technol.* **1992**, *B10*, 2422.

(25) Wróbel, A. M.; Walkiewicz-Pietrzykowska, A.; Wickramanayaka, S.; Hatanaka, Y. *J. Electrochem. Soc.* **1998**, *145*, 2866.

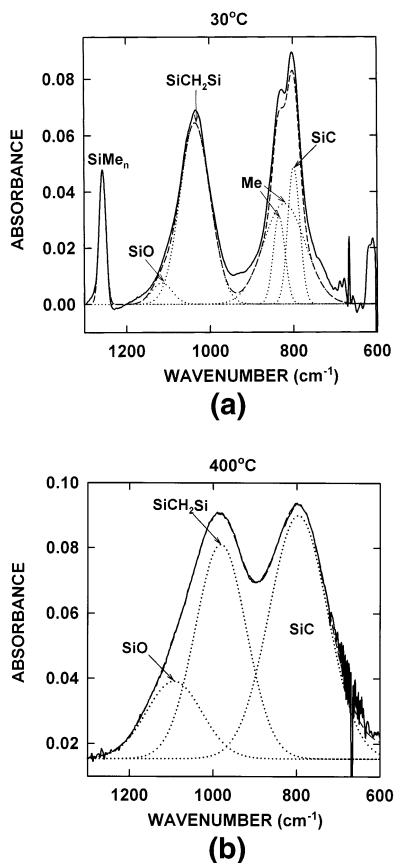


Figure 3. Deconvoluted FTIR spectra of the a-Si:C:H films deposited at the substrate temperature $T_S = 30$ and 400 °C.

band at nearly 2100 cm^{-1} , corresponding to stretching mode of the Si–H units, which is very intense in the spectrum of the DTMSM source compound at 2114 cm^{-1} . This accounts for high reactivity of a hydrosilyl unit of DTMSM with atomic hydrogen, as mentioned earlier.

The increase in the substrate temperature involves substantial changes in the film spectra. A significant drop in the intensity of absorption bands from C–H ($2960\text{--}2900\text{ cm}^{-1}$) and SiMe_n (1260 cm^{-1}) is observed. This is due to thermal scission of the C–H and Si–C bonds in the methylsilyl groups. Moreover, a marked increase in the intensity of the bands from the Si–CH₂–Si ($1040\text{--}1000\text{ cm}^{-1}$) and Si–C carbidic ($804\text{--}801\text{ cm}^{-1}$) units is noted. The latter change is associated with thermally enhanced cross-linking, which involves the formation of the carbosilane Si–CH₂–Si and Si–C carbidic cross-links.

More precise information on the evolution of film structure was obtained by the deconvolution of the IR absorption envelopes in Figure 2 (ranging from 1300 to 600 cm^{-1}) into the component absorption bands. This is exemplified in Figure 3, which shows the deconvoluted FTIR spectra of the films produced at two widely differing substrate temperatures $T_S = 30$ and 400 °C. Both spectra include the component bands from the Si–O ($1116\text{--}1098\text{ cm}^{-1}$), Si–CH₂–Si ($1035\text{--}981\text{ cm}^{-1}$), and Si–C ($799\text{--}795\text{ cm}^{-1}$) units, and the spectrum of $T_S = 30$ °C shows also the presence of the component bands from the SiMe_n (1257 cm^{-1}) and Me (835 and 822 cm^{-1} from the rocking mode in SiMe_n) units.

The oxygen contamination, as revealed by contribution of the Si–O component band, may originate from

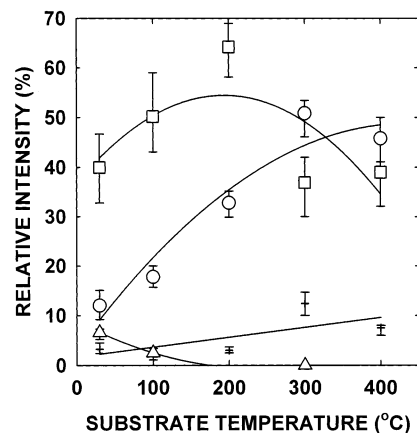


Figure 4. Relative integrated intensity of the FTIR absorption bands from the SiCH₂Si (□), SiC (○), SiMe_n (Δ), and SiO (+) units as a function of the substrate temperature.

Table 1. XPS Core Level Data for the a-Si:C:H Films Deposited at the Substrate Temperature $T_S = 30\text{--}400$ °C

core level	band no.	binding energy (eV)	fwhm	origin
Si 2p	1	99.7 ± 0.3	1.7	Si–H, Si–Si
	2	100.8 ± 0.2	1.7	Si–C (carbodic)
	3	102.0 ± 0.2	1.8	Si–O, Si–O–C
C 1s	1	283.2 ± 0.1	1.6	C–Si
	2	284.4 ± 0.2	1.6	CH _n ($n = 1\text{--}3$), C–C
	3	285.6 ± 0.1	1.8	C–O–Si
O 1s	1	532.4 ± 0.2	1.8	O–Si, O–C, C–O–Si

two potential sources. The first source may be the etching of the glass walls of the CVD system with the atomic hydrogen during RHP-CVD⁶ and resulting incorporation of the oxygen-containing etching product into the growing film. The second source is presumably reactions of the dangling bonds present in the deposit with the atmospheric oxygen or moisture, which may occur after the film exposure to the ambient.

The relative integrated intensities of the component, Si–CH₂–Si, Si–C, and Si–O bands determined as their integrated areas, are shown in Figure 4 in a function of the substrate temperature. The rise of the SiCH₂Si absorption intensity noted in the range $T_S = 30\text{--}200$ °C with simultaneous decay of the SiMe_n absorption results from the conversion of the methylsilyl units into the carbosilane Si–CH₂–Si linkages. Moreover, the drop in the intensity of the Si–CH₂–Si band observed with rising T_S in the range of $200\text{--}400$ °C is accompanied by an increase in the intensity of the band from the Si–C units. This is associated with thermally enhanced cross-linking, which involves the conversion of the Si–CH₂–Si linkages into carbosilane units with tertiary and quaternary carbon atoms, that is, Si₃CH and Si₄C, respectively.⁶ Intensity of the Si–O band is only slightly affected by T_S and remains at the low level.

The evolution of the FTIR spectra with increasing T_S similar to that in Figure 2 was observed for the a-Si:C:H films produced by RHP-CVD from hexamethyldisilane⁹ and tetrakis(trimethylsilyl)silane⁶ as well as by DP-CVD from tetramethylsilane²⁹ and tetraethylsilane.³⁰

X-ray Photoelectron Spectroscopy. The broad scan XPS spectra of the investigated a-Si:C:H films revealed the presence of distinct bands originating from the Si 2p, Si 2s, C 1s, and O 1s core levels. The high-resolution XPS data obtained for the films deposited at various

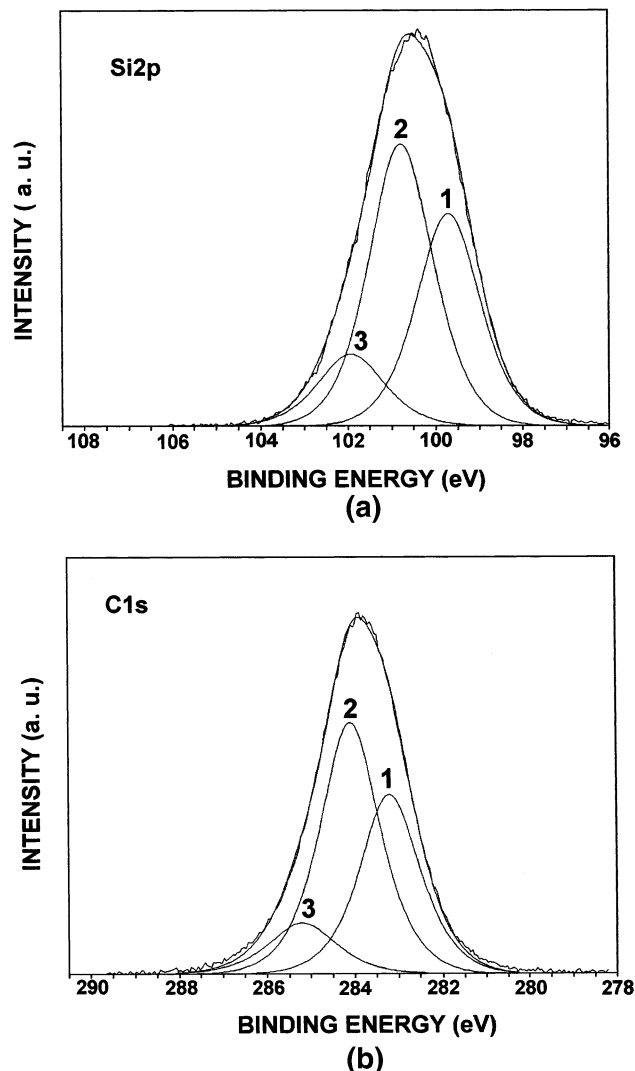


Figure 5. XPS spectra of Si 2p and C 1s core levels of the a-Si:C:H film deposited at the substrate temperature $T_S = 30$ °C.

substrate temperatures are summarized in Table 1, which specifies the binding energy of particular bands, their full-width at half-maximum (fwhm) mean values and origins. The Si 2p and C 1s spectra exemplified in Figure 5 for the a-Si:C:H film deposited at $T_S = 30$ °C are resolved into three silicon and three carbon component bands, respectively. The assignment of the particular bands in these spectra was based on the XPS literature data,^{6,33,35–40} referring to the a-Si:C:H films produced by various CVD techniques. The component bands, Si 2p at 100.8 eV (no. 2) and C 1s at 283.2 eV (no. 1), are indicative of the Si-carbidic structure in the a-Si:C:H film. The band at 284.4 eV (no. 2) in the C 1s

(35) Suzuki, Y.; Meikle, S.; Fukuda, Y.; Hatanaka, Y. *Jpn. J. Appl. Phys.* **1990**, *29*, L663.

(36) Suzuki, H.; Araki, H.; Noda, T. *Jpn. J. Appl. Phys.* **1993**, *32*, 3566.

(37) Clavaguera-Mora, M. T.; Rodriguea-Viejo, J.; El Felk, Z.; Hurtos, E.; Berberich, S.; Stoemenos, J.; Clavaguera, N. *Diamond Relat. Mater.* **1997**, *6*, 1306.

(38) Choi, W. K.; Ong, T. Y.; Tan, L. S.; Loh, F. C.; Tan, K. L. *J. Appl. Phys.* **1998**, *83*, 4968.

(39) Wang, L.; Xu, J.; Ma, T.; Li, W.; Huang, X.; Chen, K. *J. Alloys Compd.* **1999**, *290*, 273.

(40) Yoon, H. G.; Boo, J.-H.; Liu, W. L.; Lee, S.-B.; Park, S.-C.; Kang, H.; Kim, Y. *J. Vac. Sci. Technol.* **2000**, *A18*, 1464.

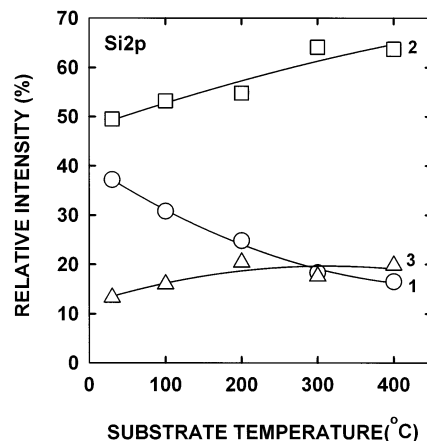


Figure 6. Relative integrated intensity of the XPS component bands in the Si 2p envelope, corresponding to (1) Si–H and/or Si–Si, (2) Si–C carbidic, and (3) Si–O units, as a function of the substrate temperature.

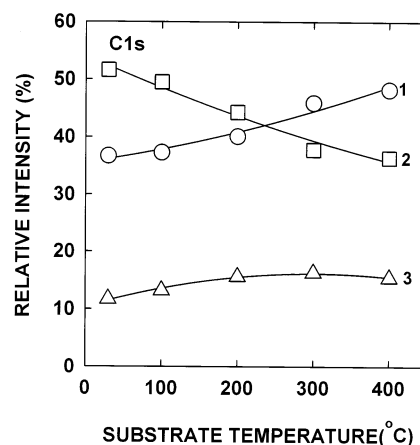


Figure 7. Relative integrated intensity of the XPS component bands in the C 1s envelope, corresponding to (1) C–Si, (2) CH_n , and (3) C–O–Si units, as a function of the substrate temperature.

envelope originates from the presence of the CH_n unit in the a-Si:C:H structure and from adventitious hydrocarbon nearly always present at any surface. The binding energy observed for this band, 284.4 eV (Table 1), differs by 0.4 from the reference value at 284.8 eV. Similar shifts, presumably due to the charging effect, we have also noted in the XPS spectra of the a-Si:C:H films produced by RHP-CVD⁵ from $(Me_3Si)_4Si$ and DP-CVD³⁴ from the $C_2H_4-SiH_4-H_2$ source mixture. The band Si 2p at 99.7 eV (no. 1) is assigned to the Si–H and/or Si–Si. However, this band seems to originate predominantly from the Si–H unit, which may be incorporated from the DTMSM source compound. This is consistent with our earlier Raman spectroscopic examination of a-Si:C:H produced by RHP-CVD from the $(Me_3Si)_4Si$ source, which revealed the absence of the Si–Si units in the film.⁶ The low-intensity bands, Si 2p at 102.0 eV (no. 3) and C 1s at 285.6 eV (no. 3), correspond to the Si–O–C and C–O–Si units, respectively. The O 1s band at 532.4 eV is ascribed to the C–O–Si unit.

Figures 6 and 7 show the relative integrated intensity of the particular bands in the Si 2p and C 1s core-level spectra, respectively, as a function of T_S . From data in Figure 6 presenting the intensity curves of the Si 2p

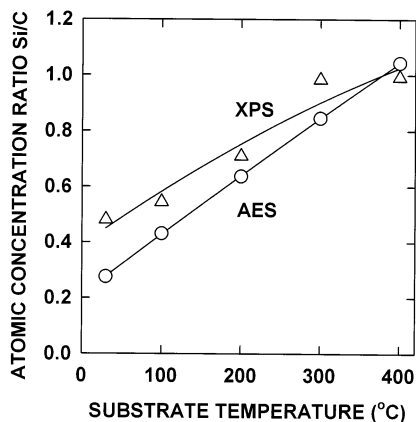


Figure 8. Atomic concentration ratio Si/C as a function of the substrate temperature determined for the a-Si:C:H film by XPS (Δ) and AES (\circ).

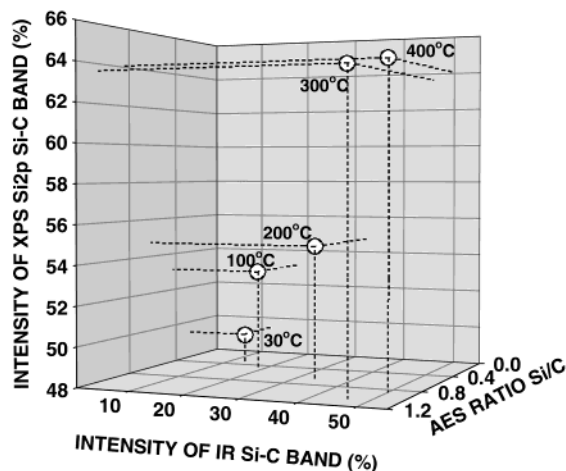


Figure 9. Correlation between the relative integrated intensities of the IR Si-C band (data from Figure 4) and the XPS Si-C band (data from Figure 6) and the AES atomic ratio Si/C (data from Figure 8) controlled by the substrate temperature.

bands, it is evident that the increase of T_S gives rise to the concentration of Si-C carbidic units (curve 2) while the content of Si-H and/or Si-Si (curve 1) is seen to decrease. Curve 3 indicates a small rise of the content of Si-O units, which gains a constant level for $T_S \geq 200$ °C. The C 1s band intensity data in Figure 7 reveal an increase in the concentration of C-Si (curve 1) and drop in the content of CH_n (curve 2) with rising T_S . A slight increase in the content of the C-O-Si units (curve 3) in the range $T_S = 30$ – 200 °C is also noted.

The trends observed in the FTIR and XPS band intensity curves in Figures 4, 6, and 7 are generally consistent and account for a large content of the Si-carbidic units in the structure of the a-Si:C:H film produced in a high T_S regime.

3.3. Film Composition and Its Correlation with Structural Data. Composition of the a-Si:C:H films is characterized by the atomic concentration ratio Si/C as the principal stoichiometric parameter, which is very sensitive to the cross-link density in the film.²² Moreover, our earlier study of the a-Si:C:H films formed by RHP-CVD from hexamethyldisilane⁸ and tetrakis(trimethylsilyl)silane⁶ revealed that the parameter Si/C (controlled by T_S) remains in close relation with hydrogen content in the film. An increase in the atomic ratio Si/C was accompanied by a drastic drop in the H

content.^{6,8} The structural changes presented in Figures 2, 3, and 8 allow one to assume a similar relation between the H content and the parameter Si/C for the examined a-Si:C:H films.

The atomic ratio Si/C determined by XPS and AES as a function of the substrate temperature is presented in Figure 8. As can be noted in this figure, the XPS and AES atomic ratios Si/C increase with rising substrate temperature reaching at $T_S = 400$ °C the values close to 1.0, which correspond to that of stoichiometric silicon carbide. Taking into account that the XPS data correspond to the surface region and the AES data refer to the bulk region, one may note from Figure 8 that the a-Si:C:H film deposited in the high substrate temperature regime displays good compositional uniformity, as revealed by very similar values of the XPS and AES ratios Si/C at $T_S = 400$ °C. We have observed for the a-Si:C:H film produced by RHP-CVD from tetrakis(trimethylsilyl)silane⁶ an analogous effect of T_S on the compositional uniformity to that in the present study.

Figure 9 shows a three-dimensional plot expressing a correlation between the structural data, that is, the relative integrated intensities of the IR Si-C band (data from Figure 4) and the XPS Si-C band (data from Figure 6), and the compositional data, that is, the AES atomic ratio Si/C (data from Figure 8), controlled by the substrate temperature. A drastic increase in the intensities of the IR and XPS Si-C bands with rising ratio Si/C again proves the elimination of organic moieties incorporated into the film from the source compound and the cross-linking via the formation of the Si-carbidic network in the deposit.

3.4. Surface Morphology. The results of the SEM study performed for the films produced at different T_S values (30, 100, 200, 300, and 400 °C) indicate that, on the micrometer scale, the substrate temperature does not influence the surface morphology of the deposit. The film surface, being very smooth and defect-free, exhibited an excellent morphological homogeneity, irrespective of the deposition temperature. The SEM images of the investigated film surfaces were almost identical to those reported for the a-Si:C:H films produced by RHP-CVD from tetrakis(trimethylsilyl)silane.^{4,6}

The surface morphology of the examined RHP-CVD films drastically differs from that of the DP-CVD films. The latter materials, and in particular those deposited in the low substrate temperature regime, often reveal a morphological heterogeneity manifested by a two-phase structure, which comprises spherical or spheroidal submicrometer powder particles embedded in a continuous film matrix.⁴¹ In light of the literature data^{41–45} reporting on the surface morphology of the DP-CVD films, the formation of powder particles is associated with the nature of the DP-CVD process and resulting initiation of the growth step in the gas phase.

(41) Wróbel, A. M.; Wertheimer, M. R. In *Plasma Deposition, Treatment, and Etching of Polymers*; d'Agostino, R., Ed.; Academic Press: Boston, MA, 1990; Chapter 3.

(42) Boufendi, L.; Bouchoule, A. *Plasma Sources Sci. Technol.* **1994**, *3*, 262.

(43) Fridman, A. A.; Boufendi, L.; Hbid, T.; Potapkin, B. V.; Bouchoule, A. *J. Appl. Phys.* **1996**, *79*, 1303.

(44) Vivet, F.; Bouchoule, A.; Boufendi, L. *J. Appl. Phys.* **1998**, *83*, 7474.

(45) Shirtcliffe, N.; Thiemann, P.; Stratmann, M.; Grundmeier, G. *Surf. Coat. Technol.* **2001**, *142–144*, 1121.

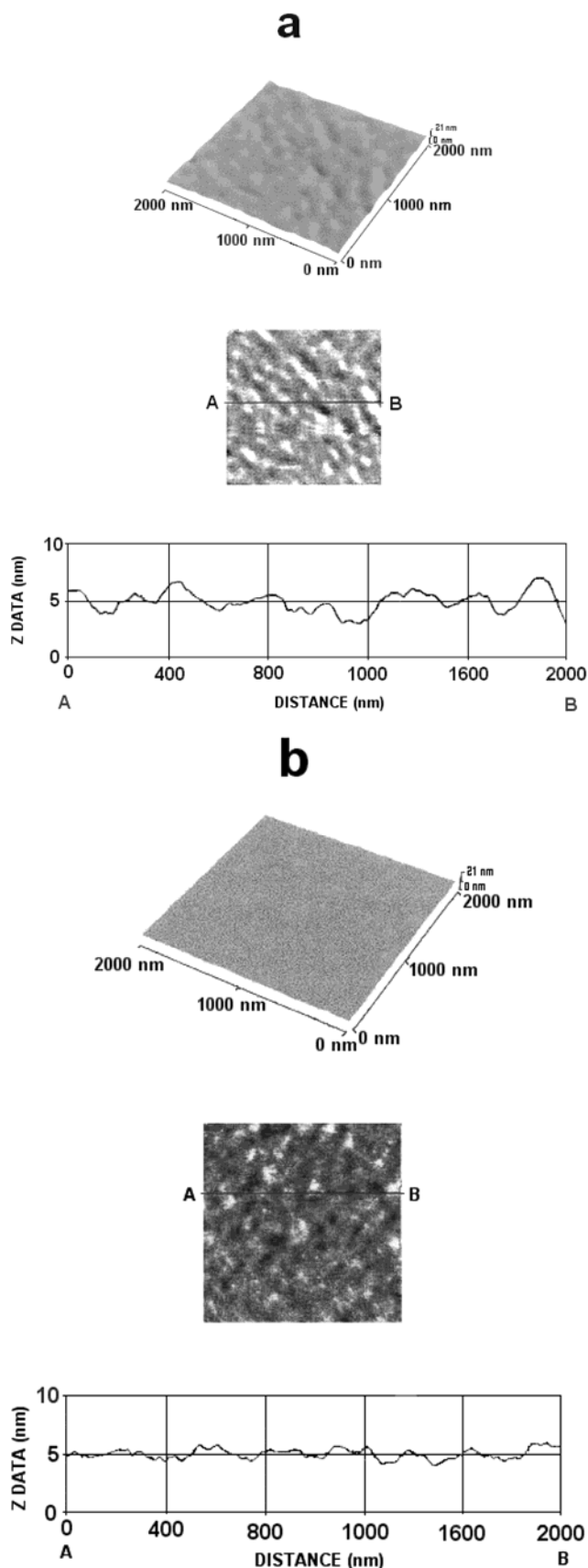


Figure 10. AFM images and cross-sectional surface profile of the a-Si:C:H film deposited at a substrate temperature of (a) 30 and (b) 400 °C.

The coalescence of the particles, which, in turn, start their own growth in the gas phase, is considered to

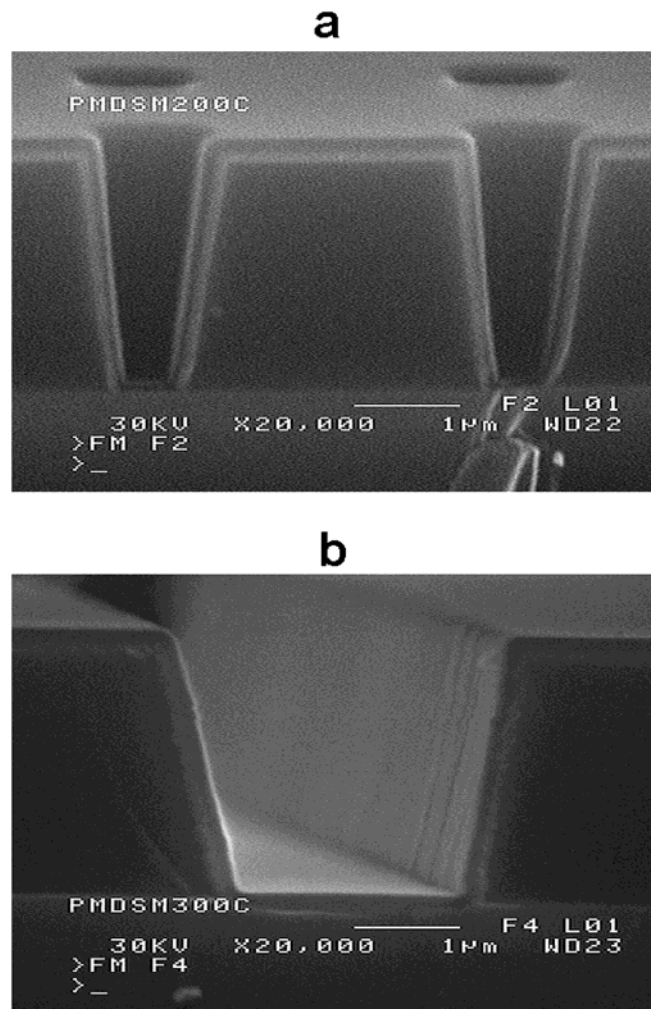


Figure 11. SEM images of cross-sectional views of the a-Si:C:H film deposited onto an Al substrate with different patterns: (a) tapered cavity ($T_s = 200$ °C) and (b) trapezoidal trench ($T_s = 300$ °C).

contribute substantially to the film formation process. The SEM data obtained in the present study, being in contrast with those of the DP-CVD films,^{41–45} suggest that the growth step in the examined RHP-CVD proceeds predominantly on the substrate surface.

Figure 10 exemplifies the AFM images and cross-sectional profiles of the surface of the RHP-CVD a-Si:C:H films deposited at two widely different substrate temperatures: 30 °C (Figure 10a) and 400 °C (Figure 10b). In contrast to the SEM data a distinct effect of this parameter on film surface morphology is observed in the nanometer scale. As can be noted from Figure 10, the increase of T_s from 30 to 400 °C involves marked smoothing of the film surface and the arithmetic mean (R_a) and root-mean-square (R_{rms}) of a surface roughness drop, R_a , from 1.4 to 0.6 nm and R_{rms} from 1.7 to 0.8 nm. This smoothing of the film surface with increasing substrate temperature may be attributed to an enhanced mobility of film-forming precursors at the growth surface, as well as to chemical processes resulting in the formation of highly cross-linked, dense material, as implied by the observed structural changes.

3.5. Conformality of Coverage. Very important useful information regarding capability of coverage of a complex profile surface by the RHP-CVD film is

provided by step coverage tests. Figure 11 shows the SEM images of the cross-sectional views of the a-Si:C:H film deposited onto an Al substrate with various patterns: tapered cavity pattern, $T_S = 200\text{ }^\circ\text{C}$ (Figure 11a), and trapezoidal trench pattern, $T_S = 300\text{ }^\circ\text{C}$ (Figure 11b). As can be noted, a thickness of the film at the bottom and sidewall surfaces of the cavity and trench is very close to that noted for the top surfaces.

The SEM data in Figure 11 demonstrate a very good conformality of coverage, which may be associated with a contribution of low-reactivity film-forming precursors, capable of rapid migration along the surface before reacting.^{25,46,47} An excellent conformality of coverage, also found for the a-SiO₂ films formed by remote oxygen plasma CVD from tetraethoxysilane,²⁵ seems to be a particularly beneficial feature of the remote plasma CVD process.

4. Conclusions

The negative values of the apparent activation energies evaluated from the Arrhenius plots of the substrate temperature dependencies of the mass- and thickness-based film growth rate suggest that the examined RHP-CVD is an adsorption-controlled process. The adsorption

of film-forming precursors onto the growth surface seems to be a major factor limiting the film growth rate.

The deposition temperature is a key parameter precisely controlling the structure and composition of the a-Si:C:H film. An increase of T_S in the low-temperature regime (30–200 °C) leads to the elimination of the methylsilyl groups SiMe_n and subsequent cross-linking via the formation of the carbosilane Si–CH₂–Si linkages. In the high T_S range (200–400 °C) dehydrogenation of the Si–CH₂–Si cross-links, resulting in the formation of the Si-carbidic network, takes place.

The a-Si:C:H films were found to be morphologically homogeneous, defect-free materials with a mean surface roughness decreasing in a relatively narrow range of values, that is, $1.4\text{ nm} \geq R_a \geq 0.6$ and $1.7\text{ nm} \geq R_{\text{rms}} \geq 0.8\text{ nm}$, with rising T_S from 30 to 400 °C. They display an excellent conformality of coverage.

In view of the presented structural data, the a-Si:C:H films are expected to display a number of interesting and useful properties, which are presented in the second part of this work.

Acknowledgment. This work was performed in a frame of the KBN research project no. 7T08C03118. The authors thank Dr. S. Lenart and Prof. M. Wysięcki (Technical University of Szczecin) for their kind assistance in the SEM examination. Special thanks are also addressed to the reviewers for valuable comments.

CM021250C

(46) Adams, A. C. In *VLSI Technology*; Sze, S. M., Ed.; McGraw-Hill: New York, 1988; Chapter 6.

(47) Sorita, T.; Shiga, S.; Ikuta, K.; Egashira, Y.; Komiyama, H. *J. Electrochem. Soc.* **1993**, *140*, 2952.